

CGCG 480-022: A DISTANT LONESOME MERGER?

C. CARRETERO¹, A. VAZDEKIS¹, A. C. GONZÁLEZ-GARCÍA¹, J. E. BECKMAN^{1,2} AND V. QUILIS³

Draft version August 1, 2006

ABSTRACT

We present a complete analysis, which includes morphology, kinematics, stellar populations and N-body simulations of CGCG 480-022, the most distant ($cz = 14317 \text{ km s}^{-1}$) isolated galaxy studied so far in such detail. The results all support the hypothesis that this galaxy has suffered a major merger event with a companion of ~ 0.1 times its mass. Morphology reveals the presence of a circumnuclear ring and possibly further ring debris. The radial velocity curve looks symmetrical, whilst the velocity dispersion increases with radius reaching values that do not correspond to a virialized system. Moreover, this galaxy deviates significantly from the Fundamental Plane and the Faber-Jackson relation. The stellar population analysis show that the ring is younger and more metal-rich, which suggest that it has undergone a fairly recent burst of star formation. Both morphological and dynamical results are in broad agreement with our N-body simulations.

Subject headings: galaxies: abundances — galaxies: individual (CGCG 480-022) — galaxies: interactions — galaxies: kinematics and dynamics — galaxies: structure — methods: N-body simulations

1. INTRODUCTION

Elliptical galaxies located in very low density environments are highly uncommon but hold important clues about galaxy formation and evolution. For example, current hierarchical models for galaxy formation predict that ellipticals in low density environments have stellar populations which are younger by 1-2 Gyr than their cluster counterparts (e.g. Baugh et al. 1998; Clemens et al. 2006; de Lucia et al. 2006). In this framework, isolated ellipticals are thought to be formed in mergers of galaxy pairs or small groups of galaxies (Jones et al. 2000; D’Onghia et al. 2005). In the first case, the mergers will give rise to kinematical misalignments whilst, in the second, they will produce an increasing amplitude of rotation with galactocentric radius, and also rotation around the minor axis (Weil & Hernquist 1996).

Detailed studies involving morphology, kinematics and/or stellar populations of isolated ellipticals have been restricted to nearby galaxies ($cz < 10000 \text{ km s}^{-1}$; e.g. Collobert et al. 2006). In this paper, we perform an exhaustive analysis of CGCG 480-022 ($cz = 14317 \text{ km s}^{-1}$), which includes morphological, kinematical, stellar population and N-body simulation properties. We present evidence supporting the hypothesis that this galaxy suffered a major merger event.

We adopt a cosmological model with $H_0 = 71 \text{ km s}^{-1} \text{ Mpc}^{-1}$, $\Omega_m = 0.3$ and $\Omega_\Lambda = 0.7$.

2. OBSERVATIONS AND DATA REDUCTION

Optical and near-IR images were extracted from the DSS and 2MASS catalogues, respectively.

Spectroscopy was obtained with the DOLORES spectrograph on the 3.5m TNG telescope at La Palma (Spain) on October 3, 2005. We used the medium-resolution MR-

B#2 grism, in the wavelength range $\lambda\lambda 3500\text{-}7000 \text{ \AA}$, and a $1.1'' \times 50''$ slit. The dispersion was 1.7 \AA/pix with an instrumental resolution of 8 \AA (FWHM). We obtained 10×30 minute exposures, interspersed with He+Ar arc-lamp spectra, flux and radial velocity standards in the same instrumental setup. The seeing was $1.1''$.

Data reduction was performed using standard IRAF packages. Once wavelength and flux calibrated, the spectra were extracted in the spatial direction coadding 4 pixels to reach the seeing size, or more if necessary to reach $S/N \geq 30$ (see Cardiel et al. 1998). Following this procedure, we obtained 13 bins out to $r = \pm 0.8 R_{\text{eff}}$.

3. ANALYSIS AND RESULTS

3.1. Morphology

To determine morphological and photometric parameters we used the code described in Trujillo et al. (2001) on K-band and optical images. Table 1 presents, for each morphological parameter, the average value obtained from both bands. Figure 1a shows the K-band image while Figure 1b shows the optical image with the spectrograph slit overplotted. According to our morphological parameters, and its optical appearance, CGCG 480-022 seems to be a typical elliptical galaxy. However, when inspecting the K-band image, we detect possible tidal tails or ring debris. In order to search for the existence of more substructures, we performed a 2D fit of the galaxy using GALFIT (Peng et al. 2002) with those parameters listed in Table 1. Figures 1c and 1d show the residuals obtained when subtracting 2D models from each image in K-band and optical, respectively. In both cases we clearly observe a well-defined ring at $r \sim 5 \text{ arcsec}$, yielding to a rippled structure similar to the shells found in other galaxies (e.g. Quinn 1984). Residuals in K-band are compatible with b-r color contours overplotted on Figure 1c.

3.2. Kinematics

The radial velocity for each bin was determined by cross-correlating the observed spectrum with a set of

¹ Instituto de Astrofísica de Canarias, Vía Láctea s/n, 38200 La Laguna, Tenerife, Spain; cch@iac.es, vazdekis@iac.es, cglez@iac.es

² Consejo Superior de Investigaciones Científicas, Spain; jeb@iac.es

³ Departamento de Astronomía y Astrofísica, Universidad de Valencia, E-46100 Burjassot, Valencia, Spain; vicent.quilis@uv.es

representative synthetic single stellar population spectra, from the model of Vazdekis (1999). This method is described in Bottema (1988), following the paper of Tonry & Davis (1979). The measured V_r values are represented versus radius in Figure 2a. Surprisingly, V_r decreases with galactocentric distance at both sides of the centre, out of 250 km s^{-1} at $r \sim 3 \text{ arcsec}$. We also see a relative increase of 100 km s^{-1} where the ring is located. Note that the plotted region represents $0.8R_{\text{eff}}$.

To measure the velocity dispersion, σ , we followed the method described in Davies et al. (1993). Figure 2b shows σ vs. radius. We observe that, within the errors, regions outside the ring present an almost constant $\sigma \sim 400 \text{ km s}^{-1}$ while the inner parts look more ordered, i.e. σ decreases, reaching 250 km s^{-1} in the centre. A similar profile has been found for the isolated massive galaxy NGC 1700 (Bergmann 2002).

3.3. N-body Simulations

To aid our understanding of these results we have performed N-body simulations. Our numerical models simulated a merger between two elliptical galaxies with a mass ratio of 10:1 and 5:1, and the fly-by of a dwarf galaxy about a massive elliptical. As initial conditions for our experiments we used: *i*) isotropic spherical Jaffe (1983) models for the elliptical galaxies, and *ii*) a King (1966) model for the dwarf galaxy, with a halo modeled with an Evans model. See González-García & van Albada (2005) for further details of this model and initial conditions for the elliptical galaxies, and Kuijken & Dubinski (1995) for the dwarf galaxy model.

We used the tree-code GADGET1.1 (Springel et al. 2001) employing 10^5 particles for each model. Low mass Jaffe models are scaled down homologous systems as the model with mass 1 and with 10 or 5 times fewer particles. Parabolic grazing orbits are employed for the merger simulations while a hyperbolic encounter is used for the fly-by experiment. Energy was well conserved, with errors well below 0.1%.

The material originally belonging to the small galaxy in the 5:1 merger finally lies on a fat disk-like distribution, while that of the 10:1 merger produces a torus-like body. The fly-by encounter produces shells and ripples in the inner parts of the giant galaxy from particles belonging to the satellite; however no ring or disk is produced in this encounter.

We have obtained a broad estimate of the mass ratio between our target galaxy and a possible companion. If we consider the merger as an inelastic collision, then the whole kinetic energy of the satellite will be transformed into ‘thermal’ energy of the stars of the main galaxy. This process will create a velocity dispersion, σ , given by $\frac{1}{2}mv_{\text{sat}}^2 = \frac{1}{2}M\sigma^2 \Rightarrow \frac{M}{m} = \left(\frac{v_{\text{sat}}}{\sigma}\right)^2$, where v_{sat} is the relative velocity of the satellite with respect to the main galaxy, and M (m) the mass of the central (satellite) galaxy. Considering that they are field galaxies, the proper motion should be of the order of $v_{\text{sat}} \sim 10^3 \text{ km s}^{-1}$, while $\sigma \sim 300 \text{ km s}^{-1}$. Then, we find $\frac{M}{m} \sim 10$. Moreover, of the models explored, the E+E 10:1 merger is the one with properties closer to those reported for CGCG 480-022. Figure 3 presents the particle distribution of the 10:1 system. A ring is clearly observable at a galactocentric distance comparable to that detected in CGCG 480-022.

The global kinematics as seen from the same point of view are given in Figure 3. The velocity curve presents a drop as we move to larger radii, in agreement with the observations, but the velocity dispersion presents a general declining profile, contrary to what is observed.

3.4. Stellar Populations

The stellar population analysis was performed following the prescriptions described in Carretero et al. (2004). To derive mean luminosity-weighted ages and metallicities, we compared selected absorption line strengths with those predicted by the model of Vazdekis (1999). This model provides flux-calibrated spectra in the optical range at a resolution of 1.8 \AA (FWHM) for single-burst stellar populations. This way, we can transform synthetic spectra to the resolution and dispersion of the galaxy spectrum. Plots of the strengths of selected indices (Mg_2 and Fe4383 ; Worthey et al. 1994) versus $\text{H}\beta$ provide close to orthogonal model grids, allowing an accurate estimation of galaxy mean age and abundances of the different elements. We have determined mean ages and relative abundances $[\text{Mg}/\text{H}]$ and $[\text{Fe}/\text{H}]$ at each galactocentric distance, computing their radial gradients.

Figure 4 presents the ages and abundances for each element with respect to the central values, versus the radial distance. If we exclude those regions within $3 < |r| < 6 \text{ arcsec}$, we observe clear gradients for both ages and abundances, with the age increasing towards outer regions and abundances decreasing throughout the galactic radius. This result is in agreement with several studies involving gradients in elliptical galaxies (e.g. Davies et al. 1993; Fisher et al. 1995; Kobayashi & Arimoto 1999).

When considering the region $3 < |r| < 6 \text{ arcsec}$, where the ring is located, we observe a decrease in age with respect to the surrounding regions, associated with a bump in metallicity. This suggests the occurrence of a star formation burst coupled with the presence of the ring.

4. DISCUSSION

The morphological, kinematical, N-body simulations and stellar population analysis all suggest that CGCG 480-022 could have experienced a major merger event with an alleged companion. In this section, we will focus on the evidences provided by each approach.

Morphology. The residuals obtained when subtracting a 2D model from the images show, in all bands, the presence of a ring of $r \sim 5 \text{ arcsec}$. This ring, together with outer streams of material appearing in K-band images, could trace the propagating sound-waves produced by a merger (e.g. Hernquist & Quinn 1987) more likely than by the action of tidal interactions or asymmetric star formation⁴ (Colbert et al. 2001). In fact, Malin & Carter (1983) found that morphological peculiarities, such as shells or ripples, occur roughly 5 times more frequently in environments outside of rich clusters. This result was confirmed by Colbert et al. (2001) who concluded that shells are much more prevalent in isolated galaxies than in group galaxies. Note that the ROSAT X-ray image of the galaxy (Zimmermann et al. 2001) shows two symmetric lobes in the N-S direction.

⁴ Even though we found a star formation burst in the ring, which would be induced by the passing wave; i.e. the varying SF history should be the effect of the ring structure, not the cause.

Kinematics. The most intriguing of our results concerns the kinematics of the galaxy. First, within the errors, we find a constant $\sigma \sim 400 \text{ km s}^{-1}$ which decreases in the interior of the ring. A similar pattern has been found in other isolated massive galaxy (NGC1700; Bergmann 2002). However, such high σ does not correspond to a virialized system but, in a merger scenario, the intrinsic velocity dispersion should be affected by the collision, yielding higher values of σ . Second, the radial velocity curve looks symmetrical. Furthermore, both σ and V_r values bump at the position where the ring is located, i.e. $3 < |r| < 6 \text{ arcsec}$. As an additional test, we checked whether CGCG 480-022 follows or not the Fundamental Plane (FP; Djorgovski & Davis 1987) and the Faber-Jackson (Faber & Jackson 1976), the Kormendy (Kormendy 1977) and the Mg_2 - σ (Terlevich et al. 1981) relations. We considered these relations in the near-IR, with data taken from Pahre et al. (1998). CGCG 480-022 deviates 3σ from the FP, 6σ from the Faber-Jackson relation and 4σ from the Mg_2 - σ relation; but just 0.2σ from the Kormendy relation. Our galaxy is an outlier in those relations involving the velocity dispersion, in the sense that it *should* be lower *if* it corresponds to the intrinsic velocity dispersion of a virialized system. Thus, a major event affecting the dynamics of this galaxy must have occurred. A similar explanation could be proposed for the V_r curve, which does *not* correspond to a rotating system. In order to disentangle the kinematical peculiarities found in this galaxy, future 2D-spectroscopy will be extremely helpful, specially to check if our derived kinematics depend on the slit direction.

N-body simulations. The N-body experiments performed suggest that a possible formation mechanism is a merger between two elliptical galaxies with a mass ratio near 10:1, and meeting each other on a grazing orbit. In such an encounter the smaller system spirals inwards while the merger is proceeding finally into a torus-like structure. Such torus as seen face-on resembles a ring and the kinematics imposed to the overall field would present a discontinuity. A significant success for this model is that it reproduces without fine tuning the velocity profile observed in CGCG 480-022. The central zones moves with a larger velocity than the zones at increasing galactocentric distances, with respect to the systemic velocity of the galaxy, and there are secondary maxima at the radial location of the ring in both directions from the center. The range of values of the velocity dispersion predicted by the model is commensurate with that observed, but the decline in value as the center is approached is not reproduced. A reasonable explanation for this is that more ordered motion near the galaxy center could result from an inner disk within the ring radius.

The present merger simulation has not, for simplicity, included the presence of gas, but merger models which do include gas (e.g. Barnes et al. 2002) show a tendency for the gas to fall towards the center of the galaxy and form a disk. Also, more detailed N-body+SPH simulations including star formation and feedback processes will help to better understand the central kinematics of the system.

Stellar populations. Following our merger hypothesis, there should be a star formation burst in the ring due to the passing sound-wave. Therefore, the stars in the ring should be younger and more metal-rich than those within inner regions, as we found. Given that we know the geometry of the ring, we can broadly estimate the crossing time of the sound-wave through the position of the ring, under the following assumptions: *i*) the sound speed is constant throughout the whole system, and *ii*) the system behaves as an ideal gas. Then, the mean pressure of a system of particles with a given velocity dispersion, σ , is $p = \frac{1}{3}\rho\sigma^2$. The propagation velocity of the perturbation corresponds to the sound speed, c_s , as $c_s^2 = \frac{dp}{d\rho} = \frac{1}{3}\sigma^2 \Rightarrow c_s \sim 180 \text{ km s}^{-1}$. Considering that the ring radius is $\sim 5 \text{ arcsec}$, then the elapsed time since the formation of the perturbation is $t(s) = 4.8 \times 10^{-6} D/c_s$, where D is the distance to the galaxy in km. Therefore, t should be the stellar age difference between the ring and the centre. Given that $D = 6.2 \times 10^{23} \text{ km}$, then $t = 5.3 \text{ Gyr}$, which is in good agreement with our stellar population results (see Figure 4). Even though approximate, these numbers do support the merger hypothesis.

A question we would like to pose is why the most distant isolated elliptical galaxy so far studied in such detail looks so peculiar. To confirm the results presented here and probe the origin of this system, deep 2D spectroscopy is strongly needed. We also note that CGCG 480-022 is not a completely isolated galaxy but has one confirmed companion at a distance of 0.25 Mpc: PGC 003298 (Beers et al. 1983). The DSS image of this galaxy shows an elongated shape in the direction of CGCG 480-022, whilst J- and K-band 2MASS images present some tail-like structures. Will PGC 003298 be the next to merge?

The authors thank S. Patiri, I. Trujillo, D. Bettoni and the referee for useful comments. AV and VQ are Ramón y Cajal Fellows of the Spanish Ministry of Education and Science. This work has been supported by the Spanish Ministry of Education and Science (grants AYA2004-03059 and AYA2004-08251-C02-01) and the Generalitat Valenciana (grant GV2005/244).

REFERENCES

- Barnes, J.E. 2002, MNRAS, 333, 481
 Baugh, C., Cole, S., Frenk, C., & Lacey, C. 1998, ApJ, 498, 504
 Beers, T.C., Huchra, J.P., & Geller, M.J. 1983, ApJ, 264, 356
 Bergmann, M. 2002, PhD Thesis, University of Texas at Austin
 Bottama, R. 1988, A&A, 197, 105
 Cardiel, N., Gorgas, J., Cenarro, J., & González, J.J. 1998, A&AS, 127, 597
 Carretero, C., Vazdekis, A., Beckman, J.E., Sánchez-Blázquez, P., & Gorgas, J. 2004, ApJ, 609, 45
 Clemens, M. S., Bressan, A., Nikolic, B., Alexander, P., Annibali, F., & Rampazzo, R. 2006, MNRAS, 370, 702
 Colbert, J., Mulchaey, J., & Zabludoff, A. 2001, AJ, 121, 808
 Collobert, M., Sarzi, M., Davies, R. L., Kuntschner, H., & Colless, M. 2006, MNRAS, in press; astro-ph/0605622
 Davies, R., Sadler, E., & Peletier, R. 1993, MNRAS, 262, 650
 de Lucia, G., Springel, V., White, S.D.M., Croton, D., & Kauffmann, G. 2006, MNRAS, 336, 499
 Djorgovski, S., & Davis, M. 1987, ApJ, 313, 59
 D'Onghia, E., et al. 2005, ApJ, 630, 109
 Faber, S.M., & Jackson, R.E. 1976, ApJ, 204, 668
 Fisher, D., Franx, M., & Illingworth, G. 1995, ApJ, 448, 119
 González-García, A.C., & van Albada, T. 2005, MNRAS, 361, 1043
 Hernquist, L., & Quinn, P.J. 1987, ApJ, 312, 1
 Jaffe, W. 1983, MNRAS, 202, 995

TABLE 1
DETERMINED PROPERTIES OF CGCG 480-022

cz	m_k	$\langle \mu_k \rangle$	R_{eff}	n	e	P.A.
km/s	mag	mag/' ²	arcsec			deg
14317	11.01	19.1	13.0	3.87	0.9	89

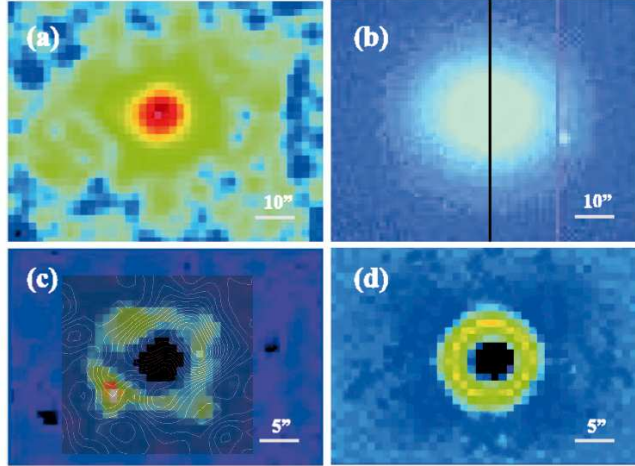


FIG. 1.— Morphology analysis. Panels (a) and (b) show the actual images of CGCG 480-022 in the K-band and optical, respectively. Panels (c) and (d) present the residuals when subtracting a 2D model of the galaxy from the images using GALFIT. In both cases, a ring of $r \sim 5$ arcsec is clearly visible. It is noteworthy that some tail-like structures appear in the outer regions of panel (a). Contours in panel (c) correspond to b-r color values. The spectrograph slit is overlotted on panel (b).

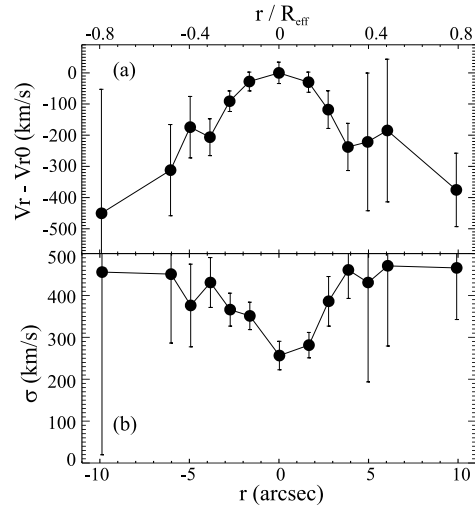


FIG. 2.— Kinematical results. *Top*: Radial velocity relative to the central value versus radius. Note that the symmetric shape does not correspond to a typical rotation curve. *Middle*: Velocity dispersion versus radius.

Jones, L., Ponman, T., & Forbes, D. 2000, MNRAS, 312, 139
 King, I. R. 1966, AJ, 71, 276
 Kobayashi, C., & Arimoto, N. 1999, ApJ, 527, 573
 Kormendy, J. 1977, ApJ, 218,333
 Kuijken, K., & Dubinski, J. 1995, MNRAS, 277, 1341
 Malin, D. F., & Carter, D. 1983, ApJ, 274, 534
 Pahre, M., Djorgovski, S., & de Carvalho, R. 1998, AJ, 116, 1591
 Peng et al. 2002, AJ, 124, 226
 Quinn, P.J. 1984, ApJ, 279, 596
 Springel, V., White, S. D. M., Tormen, G., & Kauffmann, G. 2001, MNRAS, 328, 726
 Terlevich, R.J., Davies, R.L., Faber, S.M., & Burstein, D. 1981, MNRAS, 196, 381

Tonry, J., & Davis, M. 1979, AJ, 84, 1511
 Trujillo, I., Aguerri, A., Gutiérrez, C., & Cepa, J. 2001, AJ, 122 38
 Vazdekis, A. 1999, ApJ, 513, 224
 Weil, M., & Hernquist, L. 1996, ApJ, 460, 101
 Worthey, G., Faber, S.M., González, J.J., & Burstein, D. 1994 ApJS, 94, 687
 Zimmermann, H.-U., Boller, Th., Dobereiner, S., & Pietsch, W. 2001, A&A, 378,30

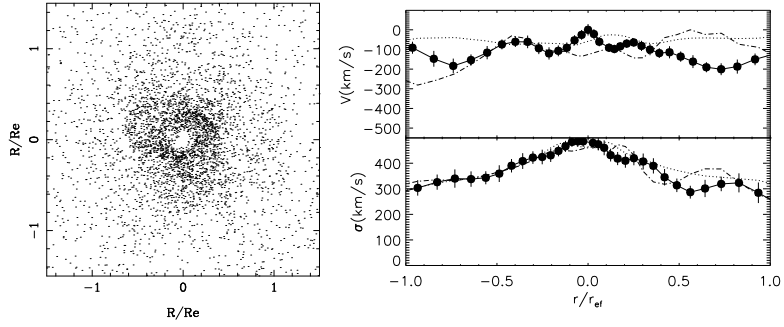


FIG. 3.— N-body results. *Left*: Material from the smaller system in the 10:1 merger remnant (for clarity, the large galaxy component is not shown). Note the presence of a well-defined ring at a galactocentric radius similar to that of the observed ring. *Right*: Kinematics for all the visible material of the merged system. Solid, dashed-dotted and dotted lines correspond to the system at 2, 2.1 and 5 Gyr after the merger, respectively. *Right-top*: Radial velocity relative to the central value versus radius. *Right-bottom*: Velocity dispersion versus radius.

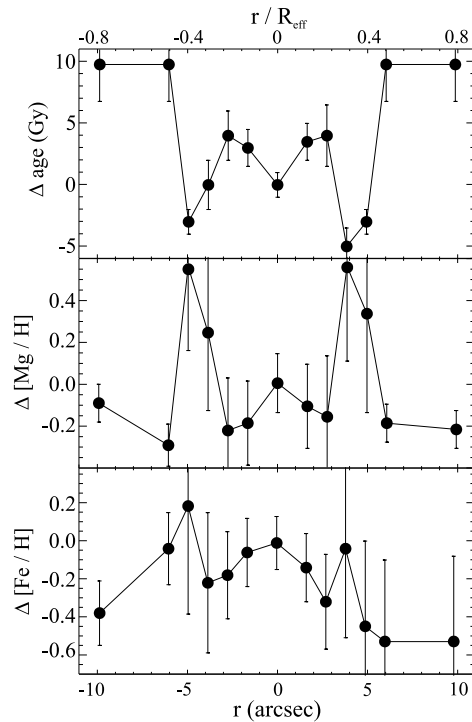


FIG. 4.— Results of the stellar population analysis. The plots show the values of the estimated ages and abundances of individual elements, relative to the centre. Expected radial gradients for both ages and metallicities are obtained if we exclude the region $3 < |r| < 6$ arcsec. At radial distances corresponding to the position of the ring, stellar population analysis indicates the presence of a recent star formation burst, with younger and more-metal rich stars.